Sensorless High-Torque Start of a Synchronous Motor using Rotor Field Polarity Inversion

Urban Lundin, Johan Abrahamsson, Fredrik Evestedt, Martin Fregelius, Jose Peréz and Jonas Kristiansen Nøland

***Abstract*—Synchronous motors are hard to line start due to torque pulsations at zero rotor speed and low starting torque when started using induced current in a damper squirrel cage. By inverting the rotor pole polarity at appropriate times it is possible to, in principle, achieve uniform torque, albeit pulsating with twice the line frequency at zero initial rotor speed. This has been demonstrated in earlier efforts. In this paper, we demonstrate that high torque starting using the back-emf in the field winding as a triggering signal for the rotor polarity inversion is possible. We further discuss the origin of the rotational energy and active and reactive power pulsations. Finally, we show that it is possible to operate a synchronous motor at continuous asynchronous speed by inverting the polarity of the rotor current and adjusting the field current accordingly, although down rated.**

***Index Terms*—AC machines, Finite element analysis, Torque control, Rotors**

I. Introduction

Synchronous motors are the high-end electrical machine of choice. Especially at higher power rating, it is the preferred product due to low losses, and less cooling requirements. On the other hand, they are relatively expensive, and it is difficult to line start them [1]. The inertia of their rotor (and mechanically connected loads) is relatively large. Therefore line start can usually not be achieved. The magnetic field of the stator rotates at a faster pace than the acceleration capabilities of the rotor. As a result, instead of accelerating, the rotor shakes. In order to overcome this impediment, a frequency converter is often utilized. The converter slowly increases the frequency of the magnetic field of the stator, allowing the rotor to follow and accelerate.

Another starting technique utilized is the asynchronous start. In order to achieve it, different methods exist, such as direct on-line (DOL), reactor start, capacitor start, autotransformer start, captive transformer start [2]. In these cases, a damper cage, or solid rotor poles, is necessary to be able to accelerate the rotor. For small motors, direct on-line (DOL) is the most common method. For large machines, 'pony' motors can also be used [3].

This work was supported in part by the StandUP for Energy.

U. Lundin, J. Abrahamsson, F. Evestedt, and M. Fregelius are with the Division of Electricity, Dept. of Engineering Sciences, Uppsala University, Box 534, SE-751 21 Uppsala, Sweden (e-mail: Urban.Lundin@Angstrom.uu.se).

J. K. Nøland is with the Norwegian University of Science and Technology.

The lack of self-starting capabilities is an undesirable characteristic that the synchronous motor shares with permanent magnet synchronous motors and synchronous reluctance motors. The fact that these types of motors are not self-starting and require a frequency converter has hindered their acceptance in applications that do not require variable speed.

In a similar way as for the synchronous motors, damper cages are utilized in permanent magnet synchronous motors and in synchronous reluctance motors to be able to achieve line start [4]–[9]. Adding a damper cage increases the initial cost of the machine and favors the utilization of the induction motor. Moreover, the failure of large motors due to broken bars is a concern [10], [11].

In an earlier work [12], we have demonstrated how rotor polarity inversion is an attractive way to achieve high torque during starting. In that work, we used a hall sensor element mounted on the pole surface as an indication of when to invert the rotor pole polarity. In this work, we extend on the previous ideas and use a sensorless technique by finite element simulations. Further, we demonstrate the possibility to operate a synchronous motor asynchronously at steady-state operation.

The remainder of the paper is organized with the following structure. Section II explains the fundamentals of field excitation from an analytical point of view. Then, the rotor polarity inversion principle is discussed in Section III. In Section IV, the case study and the finite element (FE) methodology is briefly introduced. Finally, Section V presents the main results, Section VI discussed the outcomes of the paper, before Section VII concludes the work.

II. The fundamentals of field excitation

The open-circuit dynamics of the field winding is a first order system

$$u = R_f i + L_f \frac{di}{dt}, \tag{1}$$

where R_f is the resistance, L_f the inductance, i the current and u the voltage applied over the field winding.

The general solution to this equation is

$$i = \frac{u}{R_f} + \left(i_0 - \frac{u}{R_f} \right) e^{-\frac{R_f}{L_f} t}, \tag{2}$$

where i_0 is the initial magnitude of the field current at the time the voltage is applied. Further, the corresponding rate of change of the current becomes

$$\frac{\partial i}{\partial t} = \frac{(u - i_0 R_f)}{L_f} e^{-\frac{R_f}{L_f} t}. \tag{3}$$

A. Field current control

Normally, the winding coil of each pole in the rotor is series-connected. During operation, a steady state condition with nominal field current, i_n, is achieved by applying a fraction of a relatively low ceiling voltage, u_v,

$$i_n = \frac{\gamma u_v}{R_f}, \tag{4}$$

where γ is the required fraction, as determined by an automatic voltage regulator (AVR). The fraction is typically acquired by using thyristors. Due to the relatively low maximum field voltage, the fraction γ is typically normally close to 0.5.

As a result, the current in the winding is limited by the winding resistance, and over time reaches a steady-state value when the resistive voltage drop becomes equal to the fraction of the field voltage applied. Starting from equation (3), the maximum possible rate of change of the nominal current correspondingly becomes

$$\frac{\partial i_n}{\partial t} = \frac{(1 - \gamma) u_v}{L_f}. \tag{5}$$

Another approach to field current control is to use IGBTs connected to a DC link with a significantly higher ceiling voltage, u_c. This ceiling voltage is typically around five times higher than in the previous section.

The current is controlled around its desired operating point by continuously changing the state of the switches with high frequency (typically larger than 1 kHz) as a function of a high-speed measurement of field current. The simplest, and fastest, such approach is called bang-bang control [REF].

Due to the high ceiling voltage, the controllability of the current around the nominal operating point becomes high. If even higher controllability is required, the rotor winding may be split into segments, each with dedicated switches, all connected in parallel over the same DC-link.

Under the assumption that the rotor winding is divided in N segments, the maximum possible rate of change of the current around its nominal operating point becomes

$$\frac{\partial i_n}{\partial t} = \frac{N u_c - i_n R_f}{L_f}. \tag{6}$$

For a system where u_c is five times higher than u_v and the rotor further is divided into 4 parallel subsections, each with individual current control, the rate of change of the nominal field current is increased by 18 times.

III. Field current polarity inversion

With the very high possible rate of change of the field current, comes the possibility of *motor start by field current polarity inversion*. Throughout this paper, it will be assumed that the field winding of the synchronous machine under investigation is equipped with a voltage source converter, and that the rotor winding is subdivided into N parallel subsections. Splitting the rotor circuit in several segments reduces the DC-voltage needed to invert the rotor polarity.

A. Fundamental concept

The operating principle of starting is to change the rotor polarity as the stator MMF passes the rotor pole d-axis. This means that as the torque normally would change from positive to negative the polarity switch changes the negative bell to positive at a point when the torque is naturally zero, or close to zero. The trick is to identify the point when the stator MMF is positioned at the d-axis.

The operational principle is illustrated in Fig. 1.

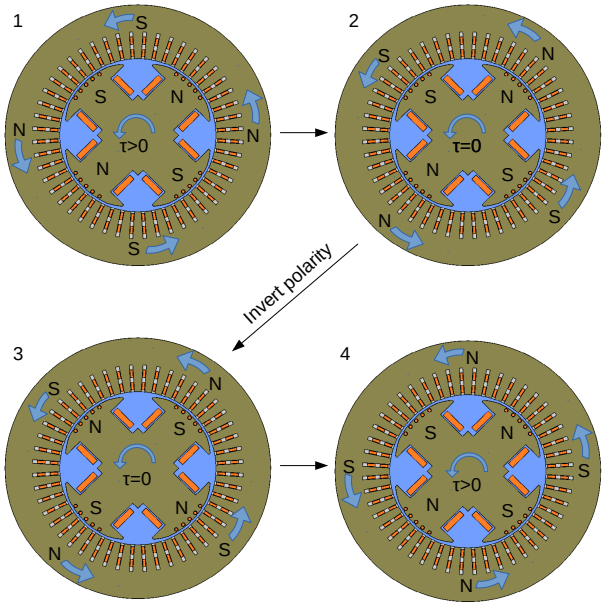

Fig. 1. Principle to achieve uniformly directed torque via rotor pole inversion. The stator MMF is rotating counter clockwise. τ indicates the sign in the same direction as the rotating armature field.

The trick is to distinguish when to invert the rotor field polarity. In Fig. 2 the contribution to the total field is shown from the armature and field windings. In the previous demonstration a flux sensor mounted on a pole was used to determine the position of the stator MMF peak. The field from the rotor had to be subtracted in the controller.

We can also observe from Fig. 1 that the induced voltage in the field winding in position 2 and 3 would be zero. So a "sensor less" control would be to use this as a signal for the armature MMF position.

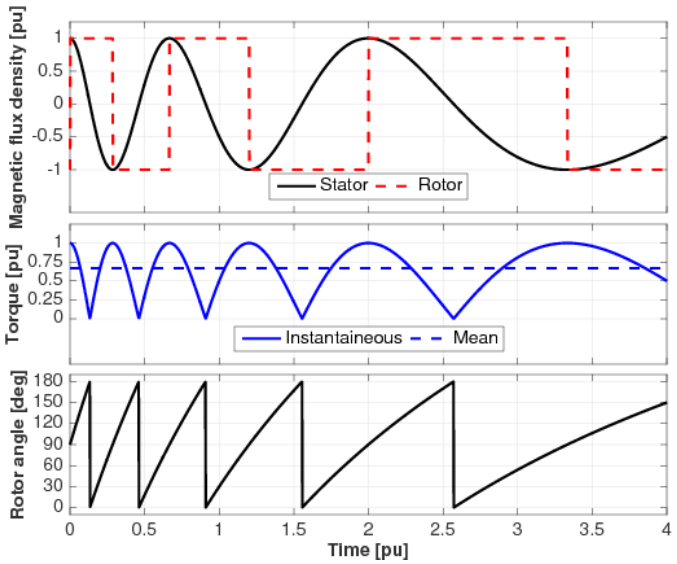

Fig. 2. Illustration of magnetic flux density contributions from the rotor and the stator during polarity inversion. The rotor is accelerated. Also, starting torque and rotor angle is shown.

B. Polarity reversal time

Since the field winding of the machine typically has a rather large inductance, the required reversal time needs to be calculated.

It should be noted that the reversal takes place around the points in time when the voltage induced in the rotor winding from the stator passes a zero crossing. This indicates that the stator MMF is passing the rotor d-axis. The effect of the EMF in the rotor has therefore been neglected. If it would be considered, it would be symmetric around the zero crossing - helping the DC-link to push the current upwards during half the reversal time, and hindering it with the same amount during the other half, resulting in the same total time as calculated below.

Fig. 2 presents the ideal hypothesis of the polarity inversion. From equation (2), it can be seen that the total time, t_s, it takes to change the current from a certain negative value, $-i_s$, to the corresponding positive value is

$$t_s = 2\frac{L_f}{R_f}\ln\frac{Nu_c}{Nu_c - R_f i_s}. \tag{7}$$

This is thereby the time required for a polarity reversal of the current. The resistive voltage drop is typically small compared with the DC-link voltage, and the natural logarithm may be expanded in a Taylor series, resulting in

$$t_s = 2\frac{L_f}{R_f}\left(\frac{R_f i_s}{Nu_c} + \frac{1}{2}\frac{R_f^2 i_s^2}{N^2 u_c^2}\cdots\right) \approx \frac{2L_f i_s}{Nu_c}. \tag{8}$$

It can be noted that, to a first approximation, the only machine parameter limiting the time required for the polarity inversion is the inductance of one rotor segment.

The time available to perform the polarity inversion should never exceed half the period of the relative electrical frequency between the rotor and the stator, in order for the resulting torque to be continuously positive. This requirement may limit the available field current, in particular during the first part of the starting phase.

$$i_{max} < \frac{Nu_c\pi}{2L_f(\omega_g - \omega_r)}, \tag{9}$$

where ω_g and ω_r are the electrical frequencies of the grid and rotor, respectively. At the beginning of the start, the rotor is stationary and relative electrical frequency equals the frequency of the grid. Assuming a 50 Hz grid frequency, this would leave 10 ms for the inversion process.

As an example, consider a 10-pole synchronous motor of 5 MW with a rated field current of 220 A, a field winding resistance of 0.7 Ω and field winding inductance of 64 mH. The field current at start would be limited to 47 A - only 21 % the of rated current, which could make accelerating the motor problematic. However, splitting the rotor windings in 5 segments with each segment being individually controlled by its own H bridge, would increase the possible starting current in the field winding up to 235 A.

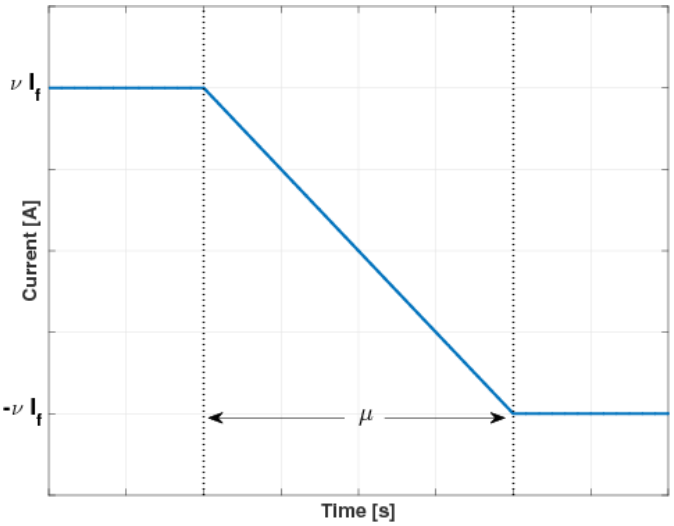

Fig. 3. Illustration of the linearized hypothesis the field polarity inversion from positive to negative field current.

IV. Method

In a previous paper the method was presented and we compared simulations with experiments done on a experimental setup. Here, only simulations were made.

Simulations were performed in an in-house 2D finite element code. The code has been verified against the physical synchronous machine that all the testing was done on. A 2D model is sufficient for the accuracy needed here, as the results are qualitative more than quantitative. The mesh is more detailed at places of interest and importance, such as the airgap. The geometry and mesh is shown in Fig. 4.

The details of the simulated machine are presented in Tab. I.

TABLE I
Details of the simulated Synchronous Motor.

Feature	Value
Rated Power	20 MVA
cosfi	0.9
Line Voltage	6 kV
Speed	1500 rpm
Outer Stator diameter	1100 mm
Airgap	8 mm
Number of damper bars per pole	7
Inertia	5000 kgm^2

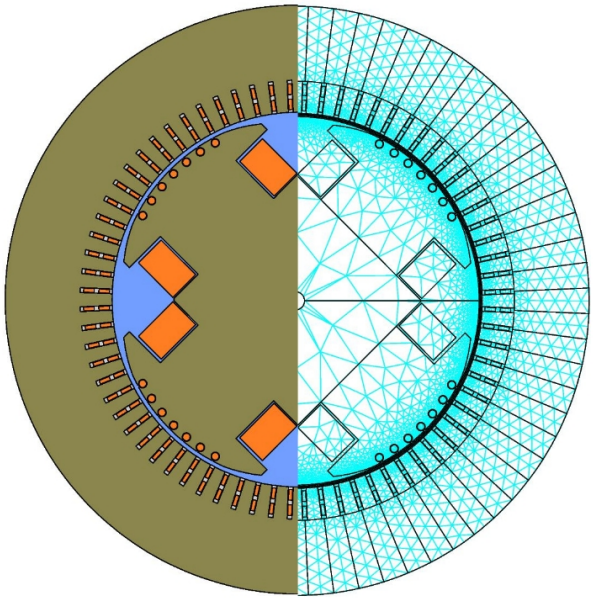

Fig. 4. The model of the motor in Finite element. The mesh contains 20'378 elements.

V. Results and Discussion

This section presents selected results of the synchronous motor starting scheme in comparison with the conventional damper start. In addition, we show new possibilities on how the motor starting technique is applicable for asynchronous speed operation.

A. Synchronous motor starting

Fig. 5 illustrates the shaking nature of the shaft torque and the grid oscillatory power under damper start operation. The shaking originates from the reluctance torque which is substantial for a salient pole machine, like the one studied here. It causes a slow rate of change in the rotational frequency of the rotor. Note that only a small amount of rotational energy is absorbed by the rotor during the shown time frame.

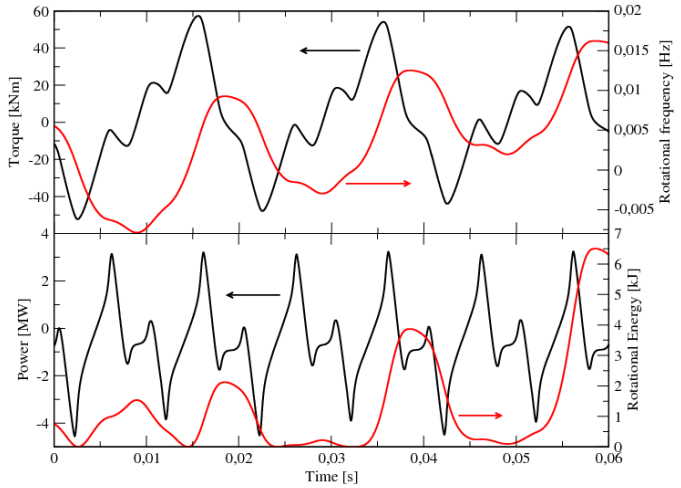

Fig. 5. Simulation results from the damper bar starting. The top graph shows the airgap torque and the rotational frequency. The inrush current gives a negative torque initially. The lower graph shows the power taken, and pushed back, to the grid during the startup, and the energy that is transferred to kinetic rotational energy.

On the contrary, Fig. 6 visualizes a smoother behavior of the active power and the accelerating torque by employing the field polarity inversion method. Note that the torque starts initially with a positive value.

It is evident that both methods express clear differences in both mechanical and electrical performance. The pulsations in the power factor angle at 12 times f_0 of the damper start is addressed in Fig. 7. The same phenomena is observed in the reactive power oscillations. In addition, the consumption of reactive power can be seen in the dc bias of the waveform. In contrast to damper start, Fig. 8 shows how the field inversion reduces the frequency of the electrical pulsations. All parameters are still pulsating, but at at a reduced frequency. The dc bias of the reactive power is reduced, whereas the dc bias of the absorbed active power is increased. Moreover, the reduced oscillatory behavior explains the reduced losses of pole inversion as shown in Table II. It compared with asynchronous operation which is expanded on in the next subsection.

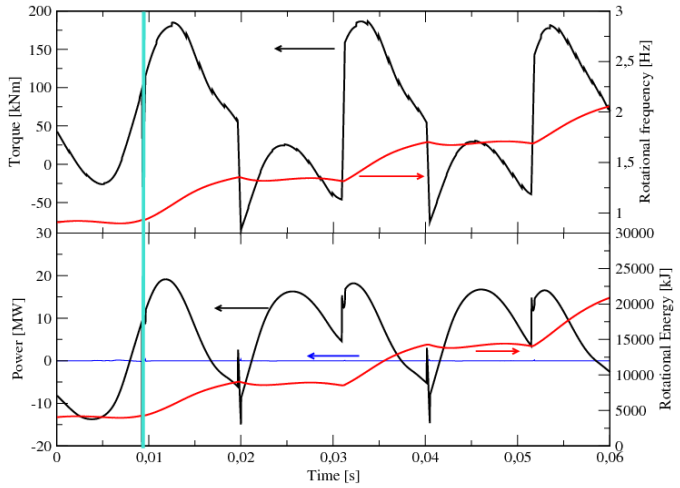

Fig. 6. Simulation results from the starting using the rotor polarity inversion. The top graph shows the airgap torque and the rotational frequency. The lower graph shows the power taken, and pushed back, to the stator (black) during the startup, the energy that the magnetization equipment for the rotor contributes with (blue), and the energy that is transferred to kinetic rotational energy. The vertical green line represents the first rotor pole inversion.

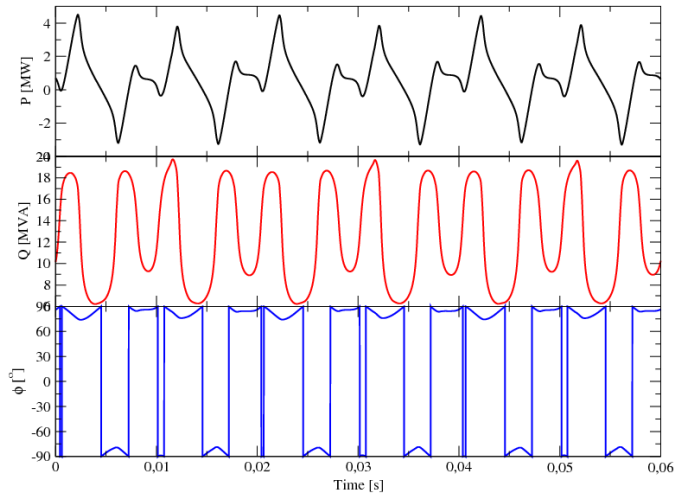

Fig. 7. The absorbed active and reactive power, and the angle between the voltage and current during a start on the damper bars.

B. Asynchronous operation of a synchronous motor

The possibility to control the torque by means of changing the amplitude of the field current means that there is also a possibility to operate a synchronous motor at asynchronous speed. This means that the rotor is under constant, changing, slip and the polarity change occurs at the same point in time as when the motor is started as described above.

A PI-controller adjusts the field current to maintain the rotational speed at the required value.

The asynchronous operation can be described as a continuous pole-slip that is "reset" at times in order to avoid the machine falling out of phase. Since the achievable torque at lower electrical frequency is lower than rated we set a target 50% of the rated power at 80% of the rated speed.

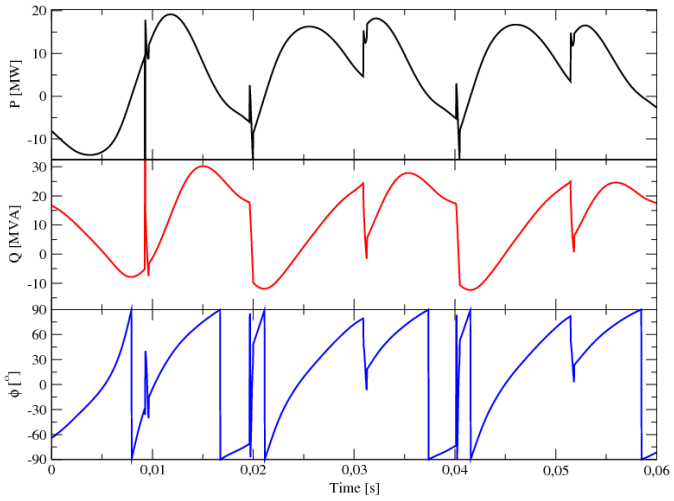

Fig. 8. The absorbed active and reactive power, and the angle between the voltage and current during a start using the described method of rotor polarity inversion.

TABLE II
AVERAGE LOSSES DURING ONE ELECTRICAL PERIOD FOR DIFFERENT MODES OF OPERATION. THE ASYNCHRONOUS OPERATION IS AT 80% RATED SPEED AND 50% OF THE RATED POWER.

Mode	Losses [kW]
Stationary Load	275
Pole inversion Starting	230
Damper bar Starting	721
Asynchronous operation[1]	136

[1]Down rated operation.

The resulting speed is shown in Fig. 9. The PI-controller continuously adjusts the field current (which is the only parameter available to adjust the speed with) to maintain the operational speed constant, as shown in Fig. 10.

The electrical and mechanical performance of the asynchronous operation is presented in Figs. 11 and 12. The slow rate of change in the power factor angle explains the slow change in the absorbed electrical power and the shaft torque. High shaft inertia ensures that the rotational energy remains approximately constant under asynchronous operation.

VI. DISCUSSION

The fundamental theory of the polarity inversion was treated in this paper. As the behavior of the field winding is different under open-circuit conditions in contrast with loaded conditions, the change in the effective inductance of the field winding needs to be accounted for. The natural inductance L_f is typically described by

$$L_f = T'_{do} R_f, \tag{10}$$

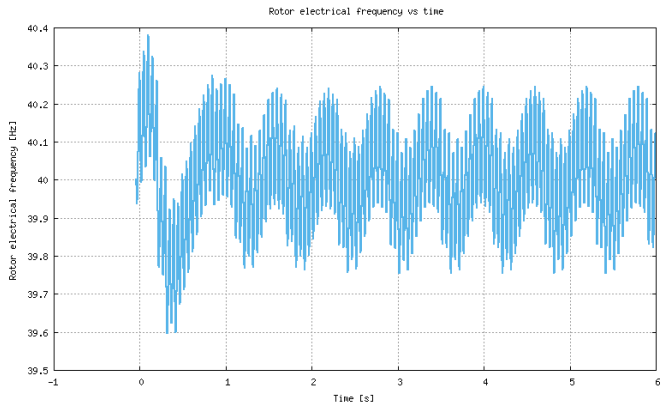

Fig. 9. Speed versus time for a synchronous machine operating asynchronously. The setpoint is 40 Hz, while the electrical frequency in the stator is 50 Hz.

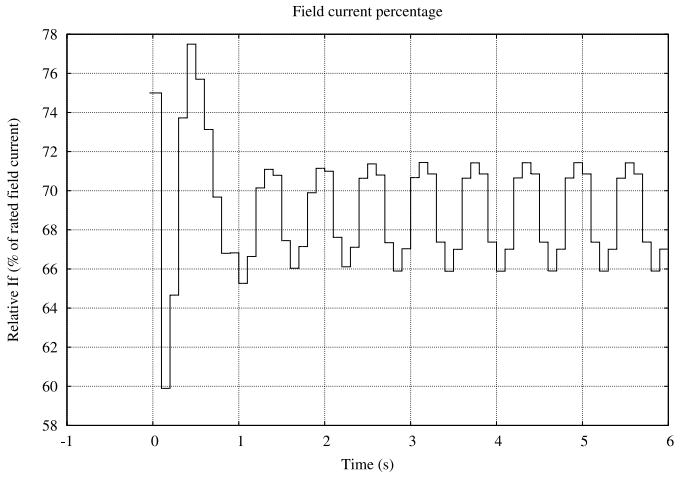

Fig. 10. Field current versus time for the asynchronous operation. The PI-controller adjusts the field current to maintain a rotor speed of 40 Hz. Since the torque is not constant there is a continuous change in the regulator setting as the rotor angle oscillates slightly.

where T'_{do} is the open-circuit time constant of the synchronous machine. However, the load time constant of the field winding is typically T'_d under loaded conditions, which are typically much lower. As a result, polarity inversion is easier to obtain under loaded conditions as compared with the open-circuit condition of the stator side.

In the experiments we have utilized current control for the rotor current. We have identified the possibility to use the switching pattern as input to the sensorless control since the back emf changes the needed switching pattern in order to maintain a certain magnetization current, and thus is a signal of the instantaneous back emf in the rotor field winding, and thereby the rotor position relative the stator MMF position.

The contribution shows that high torque starting capability of the polarity inversion as compared with the traditional

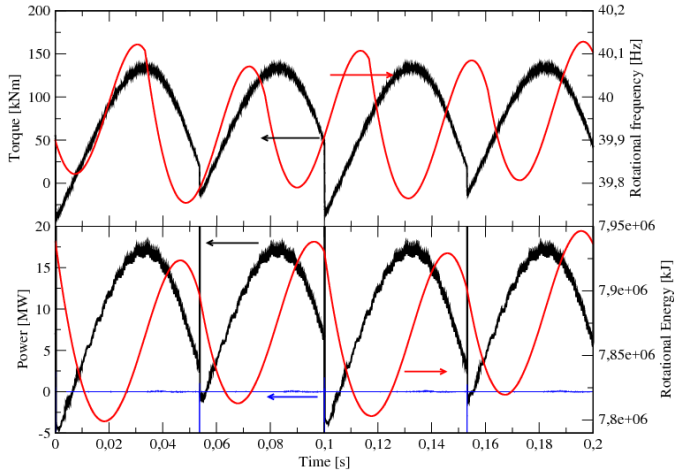

Fig. 11. Simulation results from the asynchronous operation using the rotor polarity inversion. The top graph shows the airgap torque and the rotational frequency. The lower graph shows the power taken, and pushed back, to the stator (black) during the startup, the energy that the magnetization equipment for the rotor contributes with (blue), and the energy that is transferred to kinetic rotational energy.

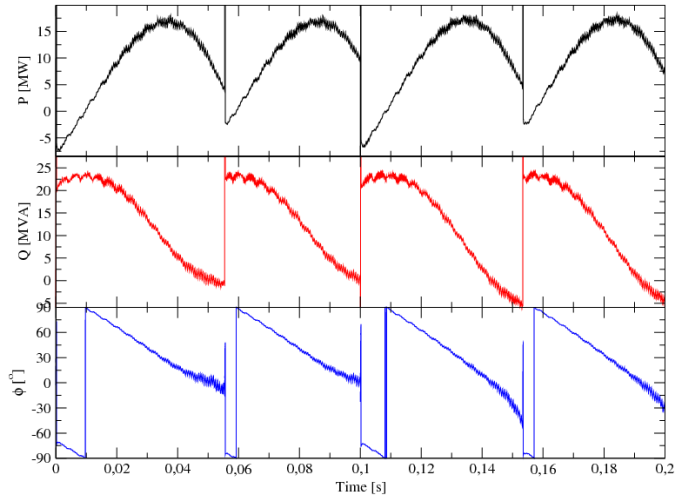

Fig. 12. The active and reactive power and the angle between the voltage and current during continuous asynchronous operation.

damper start method. In addition, reductions in electrical pulsations and reduction in losses have been shown. Moreover, the possibility for asynchronous operation by polarity inversion has been demonstrated. It shows how asynchronous speed can be achieved from the low power rotor side, rather than the high power stator side, as needed in conventional methods.

VII. Conclusion

In this paper we have shown the flow of energy during the starting of a synchronous machine. Further we have demonstrated continuous asynchronous operation of a synchronous

motor by controlling the field current, and inverting the polarity of the rotor poles.

REFERENCES

[1] R. El-Mahayni, K. Al-Qahtani, and A. H. Al-Gheeth, "Large synchronous motor failure investigation: Measurements, analysis, and lessons learned," *IEEE Trans. Ind. Appl.*, vol. 52, no. 6, pp. 5318–5326, Nov 2016.

[2] J. Nevelsteen and H. Aragon, "Starting of large motors-methods and economics," *IEEE Trans. Ind. Appl.*, vol. 25, no. 6, pp. 1012–1018, Nov 1989.

[3] K. LeDoux, P. W. Visser, J. D. Hulin, and H. Nguyen, "Starting large synchronous motors in weak power systems," *IEEE Trans. Ind. Appl.*, vol. 51, no. 3, pp. 2676–2682, May 2015.

[4] A. T. de Almeida, F. J. T. E. Ferreira, and G. Baoming, "Beyond induction motors ;technology trends to move up efficiency," *IEEE Trans. Ind. Appl.*, vol. 50, no. 3, pp. 2103–2114, May 2014.

[5] C. Debruyne, M. Polikarpova, S. Derammelaere, P. Sergeant, J. PyrhÃ¶nen, J. J. M. Desmet, and L. Vandevelde, "Evaluation of the efficiency of line-start permanent-magnet machines as a function of the operating temperature," *IEEE Trans. Ind. Electron.*, vol. 61, no. 8, pp. 4443–4454, Aug 2014.

[6] M. A. Rahman, A. M. Osheiba, K. Kurihara, M. A. Jabbar, H. W. Ping, K. Wang, and H. M. Zubayer, "Advances on single-phase line-start high efficiency interior permanent magnet motors," *IEEE Trans. Ind. Electron.*, vol. 59, no. 3, pp. 1333–1345, March 2012.

[7] R. T. Ugale and B. N. Chaudhari, "Rotor configurations for improved starting and synchronous performance of line start permanent-magnet synchronous motor," *IEEE Trans. Ind. Electron.*, vol. 64, no. 1, pp. 138–148, Jan 2017.

[8] A. Castagnini, T. KÃnsÃkangas, J. Kolehmainen, and P. S. Termini, "Analysis of the starting transient of a synchronous reluctance motor for direct-on-line applications," in *Proc. IEEE Int. Elect. Mach. Drives Conf.*, May 2015, pp. 121–126.

[9] J. Tampio, T. KÃnsÃkangas, S. Suuriniemi, J. Kolehmainen, L. Kettunen, and J. IkÃheimo, "Analysis of direct-on-line synchronous reluctance machine start-up using a magnetic field decomposition," *IEEE Trans. Ind. Appl.*, vol. 53, no. 3, pp. 1852–1859, May 2017.

[10] J. Martinez, A. Belahcen, and A. Muetze, "Analysis of the vibration magnitude of an induction motor with different numbers of broken bars," *IEEE Trans. Ind. Appl.*, vol. 53, no. 3, pp. 2711–2720, May 2017.

[11] P. J. Berry and E. S. Hamdi, "An investigation into damper winding failure in a large synchronous motor," in *Proc. Int. Univ. Power Eng. Conf.*, Sept 2015, pp. 1–4.

[12] J. J. PÃ©rez-Loya, C. J. D. Abrahamsson, F. Evestedt, and U. Lundin, "Demonstration of synchronous motor start by rotor polarity inversion," *IEEE Trans. Ind. Electron.*, vol. PP, no. 99, pp. 1–1, 2017.

VIII. BIOGRAPHIES

Urban Lundin was born in Värnamo in Sweden on 9 November 1972. He received the Ph.D. degree from Uppsala University, Uppsala, Sweden, in 2000, in condensed matter theory. He spent 2001-2004 as a Postdoc at the University of Queensland, Brisbane, Australia. In 2004, he joined the Division for Electricity at Uppsala University. He is currently a Professor in electricity with a specialisation towards hydropower systems at Uppsala University. His research focuses on synchronous generators and their interaction with mechanical components and the power system. He leads the Hydropower Group and has been involved in the industrial implementation of research projects. His current research interests include excitation systems and magnetic bearings.

Fredrik Evestedt received the M.Sc. degree in renewable electricity production from Uppsala University (UU), Uppsala, Sweden, in 2015, where he is currently working toward the Ph.D. degree in engineering physics. His main research interests include electronics, power electronics, measurement circuits, and printed circuit board design.

Johan Abrahamsson (Mâ^{TM}11) received the Ph.D. degree in engineering physics from Uppsala University, Uppsala, Sweden, in 2014. From 2014, he is a Researcher with the Division of Electricity, Uppsala University, and part of the Hydropower group. His research interests include scientific simulation, field theory, magnetic bearings, and electric drivelines.

Jose Perez received the B.Sc. degree in mechanical and electrical engineering from Tecnolgico de Monterrey, Monterrey, Mexico, in 2006, and the M.Sc. degree in electric power engineering from the Chalmers University of Technology, Gothenburg, Sweden, in 2010. He got his PhD in 2017 from Uppsala University. His research interest includes the application of magnetic forces to electrical machines.

Martin Fregelius received the M.Sc. degree in Electrical Control Systems from Uppsala University (UU), Uppsala, Sweden in 2017, where he is currently working towards the Ph.D. degree in engineering physics. His main research interests include grid tied inverters, grid stability, micro grids, power electronics, measurement circuits, and printed circuit board design.

Jonas Kristiansen Nøland received the Ph.D. degree in engineering physics from Uppsala University, Uppsala, Sweden, in 2017. He is currently an Associate Professor with the Department of Electric Power Engineering, Norwegian University of Science and Technology, Trondheim, Norway. His research interests include slotless coreless SPM machines, excitation systems, salient-pole synchronous generators, and large AC machines in the era of global energy transition. Dr. Nøland is currently serving as an Editor for the IEEE TRANSACTIONS ON ENERGY CONVERSION.